

# Investigating liquid surfaces down to the nanometer scale using grazing incidence x-ray scattering.

C. Fradin<sup>1</sup>, A. Braslau<sup>1</sup>, D. Luzet<sup>1</sup>, M. Alba<sup>1</sup> C. Gourier<sup>1,\*</sup>, J. Daillant<sup>1</sup>,  
G. Grübel<sup>2</sup>, G. Vignaud<sup>2</sup>, J.F. Legrand<sup>2,3</sup>, J. Lal<sup>2</sup>,  
J.M. Petit<sup>3</sup>, F. Rieutord<sup>3</sup>.

<sup>1</sup> Service de Physique de l'Etat Condensé, Orme des Merisiers, CEA Saclay,  
F-91191 Gif-sur-Yvette Cedex, France.

<sup>2</sup> European Synchrotron Radiation Facility, B.P. 220,  
F-38043 Grenoble Cedex, France.

<sup>3</sup> CEA/DRFMC/SI3M, F-38054 Grenoble Cedex 9, France.

June 17, 2021

*Author for correspondence:* J. Daillant,  
Service de Physique de l'Etat Condensé,  
Orme des Merisiers, CEA Saclay,  
F-91191 Gif-sur-Yvette Cedex, France.  
fax: 33 1 69 08 81 57.  
e-mail: daillant@spec.saclay.cea.fr

*Fifth international conference on surface x-ray and neutron scattering.*

## Abstract

Grazing incidence x-ray surface scattering has been used to investigate liquid surfaces down to the molecular scale. The free surface of water is well described by the capillary wave model ( $\langle z(q)z(-q) \rangle \propto q^{-2}$  spectrum) up to wave-vectors  $> 10^8 m^{-1}$ . At larger wave-vectors near surface acoustic waves must be taken into account.

When the interface is bounded by a surfactant monolayer, it exhibits a bending stiffness and the bending rigidity modulus can be measured. However, bending effects generally cannot be described using the Helfrich Hamiltonian and the characteristic exponent in the roughness power spectrum can be smaller than 4. Finally, upon compression, tethered monolayers formed on a subphase containing divalent ions are shown to buckle in the third dimension with a characteristic wavelength on the order of  $10^8 m^{-1}$ .

*Keywords:* Liquid surfaces, Surfactant monolayers.

# 1 Introduction.

The structure and dynamics of liquid surfaces and interfaces has attracted much attention since the work of van der Waals [1]. The distinctive property of liquid surfaces is a logarithmic divergence with distance of the roughness, only limited by gravity or the finite size of the surface. This behavior is well described by the capillary wave model of Buff, Lovett and Stillinger [2] which yields a height-height correlation function:  $\langle z(\mathbf{0})z(\mathbf{r}) \rangle = k_B T / (2\pi\gamma) K_0 \left( r \sqrt{\Delta\rho g / \gamma} \right)$ , where  $\mathbf{r}$  is the vector joining two points in the plane of the surface,  $\gamma$  is the surface tension, and  $\Delta\rho$  the difference in density between the two phases separated by the interface.  $K_0$  is the modified Bessel function of second kind of order 0:  $\lim_{x \rightarrow 0} K_0(x) \approx -\ln x$ . This height-height correlation function is the Fourier transform of the following spectrum:

$$\langle z(\mathbf{q})z(-\mathbf{q}) \rangle = \frac{1}{A} \frac{k_B T}{\Delta\rho g + \gamma q^2} \quad (1)$$

where  $A$  is the interface area. This spectrum has been well characterized for many liquid surfaces by light scattering down to wave-lengths in the micrometer range [3] and is valid in the limit of small in-plane momentum  $\mathbf{q}$ . The question of higher order corrections in the denominator expressing the cost in free energy related to the curvature is still open [4, 5].

Curvature effects become much more dramatic when an amphiphilic film is present at the interface because such a film may exhibit a large bending stiffness and also decreases the surface tension. In microemulsions, for instance, surface tensions as low as  $10^{-3} \text{ mN/m}$  can be achieved, and curvature effects are dominant. The simplest phenomenological model due to Helfrich [6] then predicts an additional  $Kq^4$  term in the denominator of Eq. 1. The bending rigidity  $K$  will therefore become important in limiting the out-of-plane fluctuations only at scales smaller than  $\sqrt{K/\gamma}$ , typically in the nanometer range for films spread at the air-water interface. A comprehensive understanding of the bending rigidity in terms of molecular order and chain conformations is still lacking. This is a central problem in soft condensed matter physics where systems are often composed of films (monolayers or bilayers) and the role of fluctuations is dominant. The range of situations where the Helfrich Hamiltonian can be applied is also an open question from an experimental point-of-view. Indeed, the coupling of the out-of-plane fluctuations with the fluctuation modes of any quantity of suitable

symmetry may modify the energy spectrum [7]. For example, in the case of a tethered membrane having the elasticity of a solid, there can be a coupling between out-of-plane fluctuations and in-plane modes due to the fact that many configurations of the film with low bending energy *per se* imply stretching. This leads to a divergence of  $K(q)$  at large scale, or a rigidity term in the spectrum proportional to  $1/q^{4-\eta}$ ,  $1/2 < \eta < 1$  [8, 9, 10]. Another interesting case is that of polarization for dipoles normal to the surface, always carried by classical amphiphiles, which leads to a non-trivial  $q^{-3}$  dependence[7].

The examples cited in this introduction indicate that the key problems in liquid interfaces quite generally occur at very small length-scales. The many powerful techniques used to investigate solid surfaces generally require ultra-high vacuum and cannot be applied to the study of liquid surfaces. The scattering of short wave-length radiation (x-rays or neutrons) thus provides unique information. The first reflectivity experiments on liquid surfaces were carried out on liquid metals [11, 12] in the 70's and the roughness of the free surface of water was demonstrated to be consistent with the capillary wave model in the mid 80's [13, 14, 15]. In reflectivity studies however, only density profiles averaged over the surface can be measured. From the beginning of the 90's, the analysis of diffuse scattering from the surface, which gives access to the roughness spectrum has been undertaken[16, 17]. The spectrum could be measured up to wave-vectors of the order of  $10^7 m^{-1}$ . The method has been more recently extended down to molecular length-scales giving access to new phenomena [18]. After a short presentation of the method we discuss the results concerning the bare water surface and give some examples for surfactant monolayers.

## 2 Experimental method.

Langmuir films (monolayers of insoluble amphiphiles at the air/water interface) offer the possibility of measuring the fluctuation spectra of oriented films with a well characterized structure. Temperature, molecular area or surface tension can indeed be fixed, the structure can be determined by grazing incidence x-ray diffraction and reflectivity, and the texture observed *in situ* by Brewster Angle Microscopy

or by atomic force microscopy (on transferred films). In this paper, we present direct measurements of the fluctuation spectra by grazing-incidence diffuse x-ray scattering [19, 20, 21, 22, 23, 24].

In a Langmuir film, the scattering of x-rays results from height fluctuations of the different interfaces (air/chain, chain/head, head/subphase), assumed in this study to fluctuate conformally. The interferences between beams scattered at the different interfaces, which can be accounted for within the Distorted Wave Born Approximation taking into account refraction and absorption [20, 21], give rise to the normal  $q_z$  dependence. The  $(q_x, q_y)$  dependence of the scattered intensity is concentrated in the form:  $e^{-q_z^2 \langle z^2 \rangle} \int dx dy [e^{q_z^2 \langle z(0,0)z(x,y) \rangle} - 1] e^{i(q_x x + q_y y)} \tilde{R}(x, y)$ , where  $\tilde{R}(x, y)$  is the Fourier transform of the resolution function. For small  $q_z$ , the exponential can be developed and one simply gets the convolution of the roughness spectrum  $\langle z(\mathbf{q})z(-\mathbf{q}) \rangle$  with the resolution function.

The measurements were performed at the “Troika” and “CRG-IF” beamlines of the European Synchrotron Radiation Facility (ESRF). Two types of experimental configurations were used (Fig.1). At the Troika beamline (undulator) the desired radiation was selected using the (111) reflection of a diamond monochromator in a Laue geometry. A SiC mirror was used in the monochromatic beam in order to fix the grazing angle of incidence and eliminate higher order light. At the CRG-IF beamline (bending magnet) a double Si(111) monochromator and a platinum coated glass mirror are used. In both cases, the intensity of the  $0.4 \times 0.2 \text{ mm}^2$  ( $w \times h$ ) beam was approximately  $2 \times 10^{10} \text{ counts/s}$ . The two beamlines differ notably for these experiments in the horizontal divergence of the synchrotron x-ray beam at the sample. A home-made Langmuir trough was mounted on a Nanofilm technologie GmbH active vibration isolation system on the sample stage of the diffractometer. Since the signal scattered by the interfacial fluctuations at large in-plane wave-vectors  $q_{xy}$  is very low ( $\approx 10^{-10}$  of the incident beam), extreme care was taken to limit the background by shielding of the experimental device and by a flux of He gas in the Langmuir trough. Another very important requirement is to fix the grazing angle of incidence below the critical angle for total external reflection in order to limit the penetration and therefore scattering in the bulk. Under total external reflection conditions the background could be measured by simply lowering the trough by  $1 \text{ mm}$  and scanning around the

direct beam. The first type of experiments consisted of  $\theta_d$  detector scans in the plane of incidence with a fixed angle of incidence  $\theta_i$  (see Fig.1a). With this geometry both  $q_x = 2\pi/\lambda [\cos(\theta_i) - \cos(\theta_d)]$  and  $q_z = 2\pi/\lambda [\sin(\theta_i) + \sin(\theta_d)] \approx \sqrt{4\pi q_x/\lambda}$  are varied jointly in an experiment. In a second type of experiments (Fig.1b) we measured the scattered intensity in the  $q_y$  direction, i.e. without any coupling to the vertical structure. Intensity was collected using a NaI(Tl) scintillator in the first configuration and a gas-filled (xenon) position sensitive detector (PSD) in the second configuration.

### 3 Bare water free surface.

The intensity scattered by the bare water free surface (from a Millipore purification system) is presented in (Fig.2) for both experimental configurations. In this case the scattered intensity can be calculated without *any* adjustable parameter: the surface tension  $\gamma_{H_2O}$  is known, as well as the different parameters determining the resolution of the experiment (slit dimensions, incident and accepted beam footprints). The intensity scattered in the plane of incidence is presented in Fig.2a. The data extend to  $q \geq 10^8 m^{-1}$  and are well described by the spectrum of Eq.1. The data taken in the interface plane ( $q_y$ ) extend to even larger wave-vector ( $\approx 10^{10} m^{-1}$ , note that this is more than two orders of magnitude than that of the best previous measurements [16]) but can only be described with the spectrum of Eq.1 up to  $q \approx 5 \times 10^8 m^{-1}$ . The excess scattering at  $q \geq 10^9 m^{-1}$  indicates either a smaller effective surface tension at such large wave-lengths [5] or another source of scattering. Because this scattering seems to have no dependence on  $q$  (the apparent  $q^{-1}$  dependence on Fig.2 is due to the resolution function), it can be due to acoustic waves within the penetration depth of the beam. The corresponding scattering cross-section [21] can be calculated from the density-density correlation function at or near the interface which can itself be determined by using the linear response theory [3]:

$$\frac{d\sigma}{d\Omega} = \frac{A(1 - n^2)^2 |t_{in}|^2 |t_{out}|^2 k_B T \kappa_T}{2\mathcal{I}m(q_z)}, \quad (2)$$

where  $n$  is the refraction index of water,  $t_{in}$  and  $t_{out}$  are the transmission coefficients of the air/water interface for the incident and scattering beams,  $\kappa_T$  is the isothermal compressibility of water ( $4.58 \times 10^{-10} m^2 N^{-1}$ ), and  $\mathcal{I}m(q_z)$  is the imaginary part of the normal component of the wave-vector transfer (inverse of the penetration length). Including this contribution gives a better agreement (Fig.2b), without discarding the possibility of other corrections.

## 4 Surfactant monolayers.

When a surfactant monolayer is present at the interface, its first effect is to reduce the surface tension:  $\gamma = \gamma_{H_2O} - \Pi$ , where  $\Pi$  is the surface pressure, as illustrated in Fig.3 for an arachidic acid ( $CH_3 - (CH_2)_{18} - COOH$ ) film. Higher order corrections to the spectrum, i.e. effects of the bending stiffness of the film are also evidenced. Results for a  $L_\alpha$  di-palmitoylphosphatidylcholine (DPPC) film on pure water are presented in Fig.4. Whereas at small  $q_y$  values the scattered intensity scales with the surface tension as expected, this is no longer true at large  $q_y$  due to the effect of bending stiffness. We have analysed the data of Fig.4 using the spectrum Eq.1 plus an additional term  $Kq^4$  in the denominator. For the more compressed film of Fig.4 we find  $K = (5 \pm 2)k_B T$ , smaller than generally expected in condensed DPPC films [25], but consistent with a naïve estimation relying on the theory of the elasticity of solid shells:  $K = \epsilon h^2/12 \approx 13k_B T$  with  $\epsilon \approx 0.3N/m$  [26], the inverse of the compressibility of the film of thickness  $h \approx 1.4nm$  [27]. The observed wave-vector range is not large enough to allow the precise determination on the exponent 4.

We have observed exponents smaller than 4 in the case of the very rigid films[18] formed by fatty acids (here behenic acid  $CH_3 - (CH_2)_{20} - COOH$ ) on divalent cation subphases ( $5 \times 10^{-4} mol/l CdCl_2$ ) at high pH (8.9) and low temperature ( $5^\circ C$ ). Uncompressed, such films exhibit a  $q^{-3.3}$  power law which could be due to the coupling between in-plane (phonons) and out-of-plane elasticity [18]. Under compression, those rigid films buckle in the third dimension as shown on Fig.5. The film is homogeneous at scales  $< 1\mu m$ , and the only possible source of scattering (i.e. refractive index inhomogeneities) are indeed surface corrugations. As shown in Fig.5, the buckling wave-length

$\Lambda \approx 2\pi/(3 \times 10^8 m^{-1}) \approx 20nm$  changes only slightly under compression, but the amplitude strongly increases. This buckling could be induced by the asymmetry in packing constraints for headgroups and aliphatic chains, like in the ripple phase of lyotropic liquid crystals [28] where similar periods are observed. The buckling wave-length (Fig. 5) could result from a balance between the headgroup size inducing spontaneous curvature, the chain length that would limit the possible curvature, surface tension and the energy cost of defects.

## 5 Conclusion

In conclusion, the possibility of measuring height fluctuation spectra of liquid-gas interfaces down to molecular scales, thus enabling the determination of exponents and bending constants by means of x-ray surface scattering has been demonstrated. We are currently extending this method for measurements of films at liquid-liquid interfaces.

\* *present address:* LPMI, Université de Pau, 2 av. du président Angot, F-64000 Pau.

## References

- [1] J.S. Rowlinson and B. Widom, “Molecular Theory of Capillarity” Clarendon Press, Oxford 1982.
- [2] F.P. Buff, R.A. Lovett and F.H. Stillinger Jr. *Phys. Rev. Lett.* **15** 621 (1965).
- [3] See for example R. Loudon, “Ripples on liquid interfaces” in “Surface excitations” edited by V.M. Agranovich and R. Loudon, Modern Problems in Condensed Matter Science, vol. 9, North-Holland, Amsterdam, 1984.
- [4] J. Meunier, *J. Physique* **48** 1819 (1987).
- [5] M. Niarórkowski, S. Dietrich, *Phys. Rev. E* **47** 1836 (1993).
- [6] W. Helfrich, *Z. Naturforschung* **28 c** 693 (1973).
- [7] L. Peliti and J. Prost, *J. Phys. France* **50** (1989) 1557.
- [8] D.R. Nelson and L. Peliti, *J. Phys. France* **48** (1987) 1085.
- [9] F.F. Abraham and D.R. Nelson *Science* **249** (1990) 393.
- [10] R. Lipowsky and M. Girardet, *Phys. Rev. Lett.* **65** (1990) 2893; F.F. Abraham *Phys. Rev. Lett.* **67** (1991) 1669; P. Le Doussal and L. Radzihovsky *Phys. Rev. Lett.* **69** (1992) 1209; I.B. Petsche and G.S. Grest *J. Phys. I France* **1** (1993) 1741.
- [11] B.C. Lu, S.A. Rice, *J. Chem. Phys.* **68** 5558 (1978).
- [12] L. Bosio, M. Oumezine, *J. Chem. Phys.* **80** 959 (1984).
- [13] A. Braslau, M. Deutsch, P.S. Pershan, A.H. Weiss, J. Als-Nielsen, J. Bohr, *Phys. Rev. Lett.* **54** 114 (1985).
- [14] A. Braslau, P.S. Pershan, G. Swislow, B.M. Ocko and J. Als-Nielsen, *Phys. Rev. A*, **38**, 2457 (1988).
- [15] J. Daillant, L. Bosio, B. Harzallah, J.J. Benattar, *J. Phys. France II* **1** 149 (1991).
- [16] D.K. Schwartz, M.L. Schlossman, E.H. Kawamoto, G.J. Kellog, and P.S. Pershan, *Phys. Rev. A* **41** 5687 (1990).
- [17] M.K. Sanyal, S.K. Sinha, K.G. Huang, B.M. Ocko, *Phys. Rev. Lett.* **66** 628 (1991).
- [18] C. Gourier, J. Daillant, A. Braslau, M. Alba, K. Quinn, D. luzet, C. Blot, D. Chatenay, G. Grübel, J.-F. Legrand, and G. Vignaud, *Phys. Rev. Lett.* **78** 3157 (1997).

- [19] S.K. Sinha, E.B. Sirota, S. Garoff, and H.B. Stanley, *Phys. Rev. B* **38**, 2297 (1988).
- [20] J. Daillant, O. B elorgey *J. Chem. Phys.* **97** 5824 (1992).
- [21] J. Daillant, K. Quinn, C. Gourier, F. Rieutord, *J. Chem. Soc. Faraday Trans.*, **92** 505.
- [22] S. Dietrich, A. Haase, *Physics Reports*, **260** 1 (1995).
- [23] S.K. Sinha *Current opinion in solid state and material science* **1** 645 (1996).
- [24] R.K. Thomas, J. Penfold *Current opinion in colloid and interface science* **1** 23 (1996).
- [25] E. Sackmann in “Handbook of biological physics”, vol. 1A edited by R. Lipowsky and E. Sackmann, Noth-Holland, Amsterdam, 1995.
- [26] O. Albrecht, H. Gruler, and E. Sackmann, *J. Phys. France* **39** 301 (1978).
- [27] T.M. Bayerl, R.K. Thomas, J. Penfold, A. Rennie, and E. Sackmann, *Biophys. J.* **57** 1095 (1990). *Phys. Rev. Lett.* **78** 3157 (1997).
- [28] J.M. Carlson and J.P. Sethna, *Phys. Rev. A* **36** 3359 (1987).

Figure 1: Schematics of the experiment (Troika beamline) (a):  $(q_x, q_z)$  incidence plane geometry. (b): in-plane  $q_y$  geometry.  $C^*(111)$ : diamond monochromator, SiC: mirror, VP: vacuum paths, LT: Langmuir trough, NaI(Tl): scintillation detector. PSD: position sensitive gas-filled (xenon) detector. The curve in (b) represents the scattered intensity (horizontal axis) as a function of the vertical position on the PSD.

Figure 2: Scattering by the bare water surface in the plane of incidence (a) and in the plane of the surface (b). For measurements in the plane of incidence  $q_x$  is the projection of the wave-vector transfer on the horizontal. “1mm” (circles) and “10mm” (triangles) is the opening of slit  $s_3$  in Fig.1a. Squares represent the background which was not subtracted. In (b) the background was subtracted following the procedure indicated in text. The full line is calculated by using the capillary wave spectrum of Eq.1 and the acoustic wave scattering cross section Eq.2 has been included to calculate the dashed line curve. Note that the great dynamic range of the y-scale has been compressed by a multiplication of the measured scattered intensity by  $q_x$  or  $q_y^2$ .

Figure 3: (a): Intensity scattered by an arachidic acid film (black curves) and water (grey curves). The surface tensions are (top to bottom) 33 mN/m (diamonds), 43mN/m (triangles), 53mN/m (squares), 69mN/m (circles) and 73mN/m. (b): The same data normalized by  $\gamma/\gamma_{water}$  in order to illustrate the scaling  $I \propto \gamma$  in the range  $3 \times 10^6 m^{-1} \leq q_x \leq 8 \times 10^6 m^{-1}$  where capillary waves dominate the fluctuation spectra. The fringes are due to the normal film structure since  $q_z$  is not constant in the (x,z) configuration.

Figure 4: Intensity scattered in the horizontal plane by a bare water surface (grey triangles) and a DPPC film at  $3^{\circ}C$  compressed at  $20mN/m$  (grey circles) and  $40mN/m$  (black circles). Lines are the best fits as indicated in text. Note that the scattered intensity scales with the surface tension at low  $q_y$  but that this is no longer true at large  $q_y$  due to the effect of bending stiffness (the black curve passes below the grey curves). Inset: corresponding molecular area - surface pressure isotherm.

Figure 5: Intensity scattered in the plane of incidence by an arachidic acid film deposited on a  $5 \times 10^{-4}mol/l$   $Cdcl_2$  subphase at  $pH = 8.9$  and  $T = 5^{\circ}C$ . Bottom to top,  $\Pi = 1.4mN/m, 1.8mN/m, 5mN/m, 14.6mN/m, 17.3mN/m,$  and  $20mN/m$ .

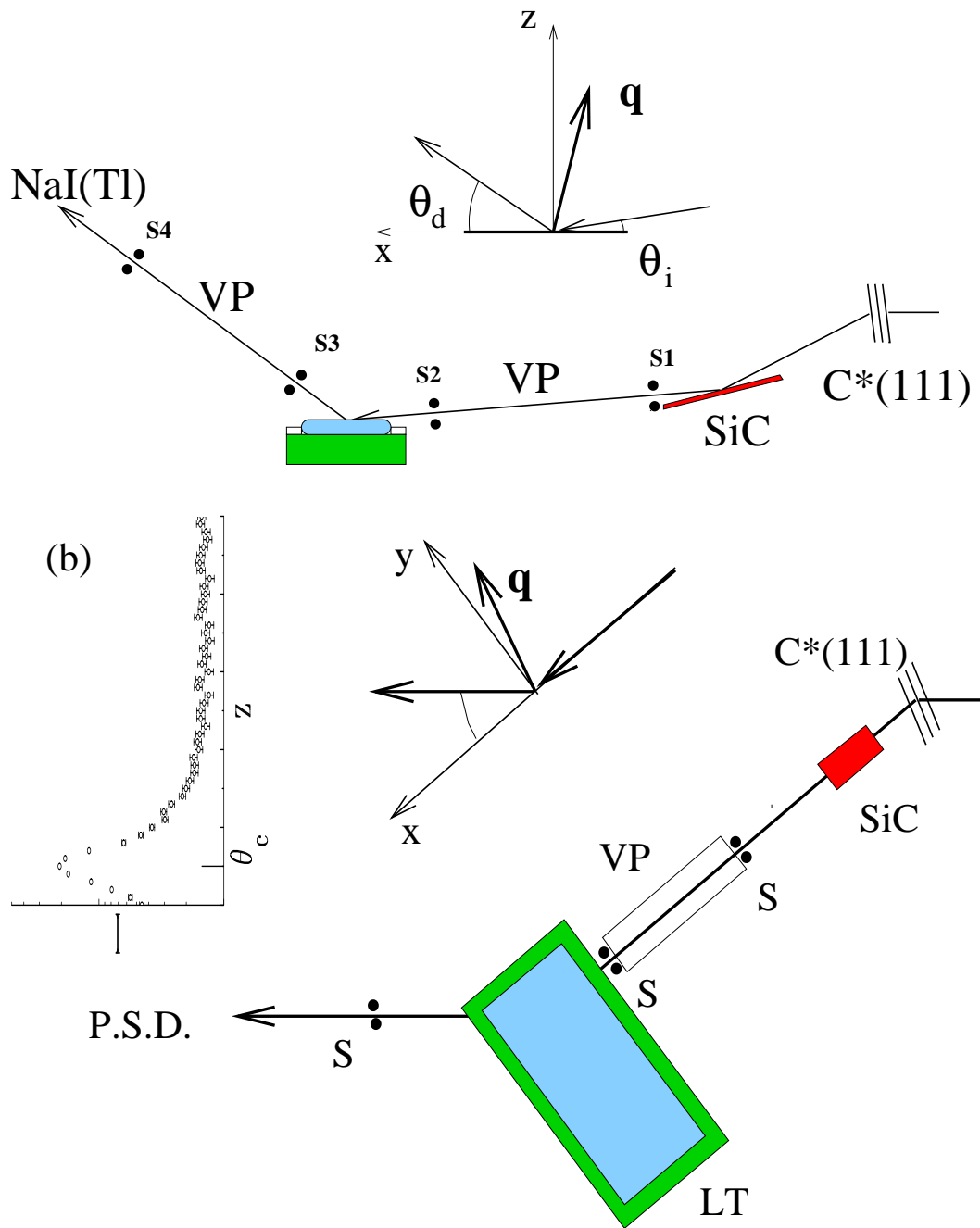


Fig. 1

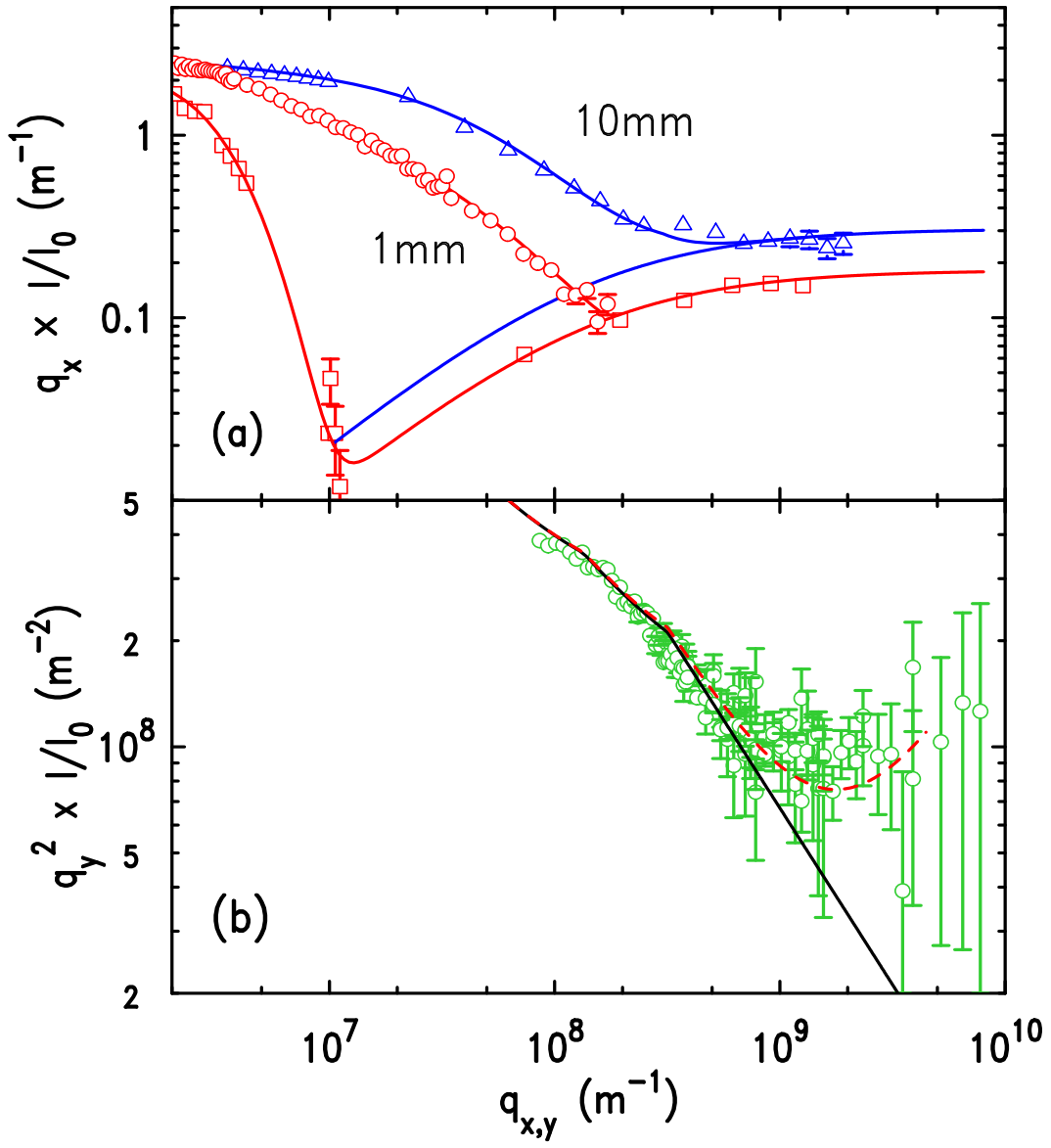


Fig. 2

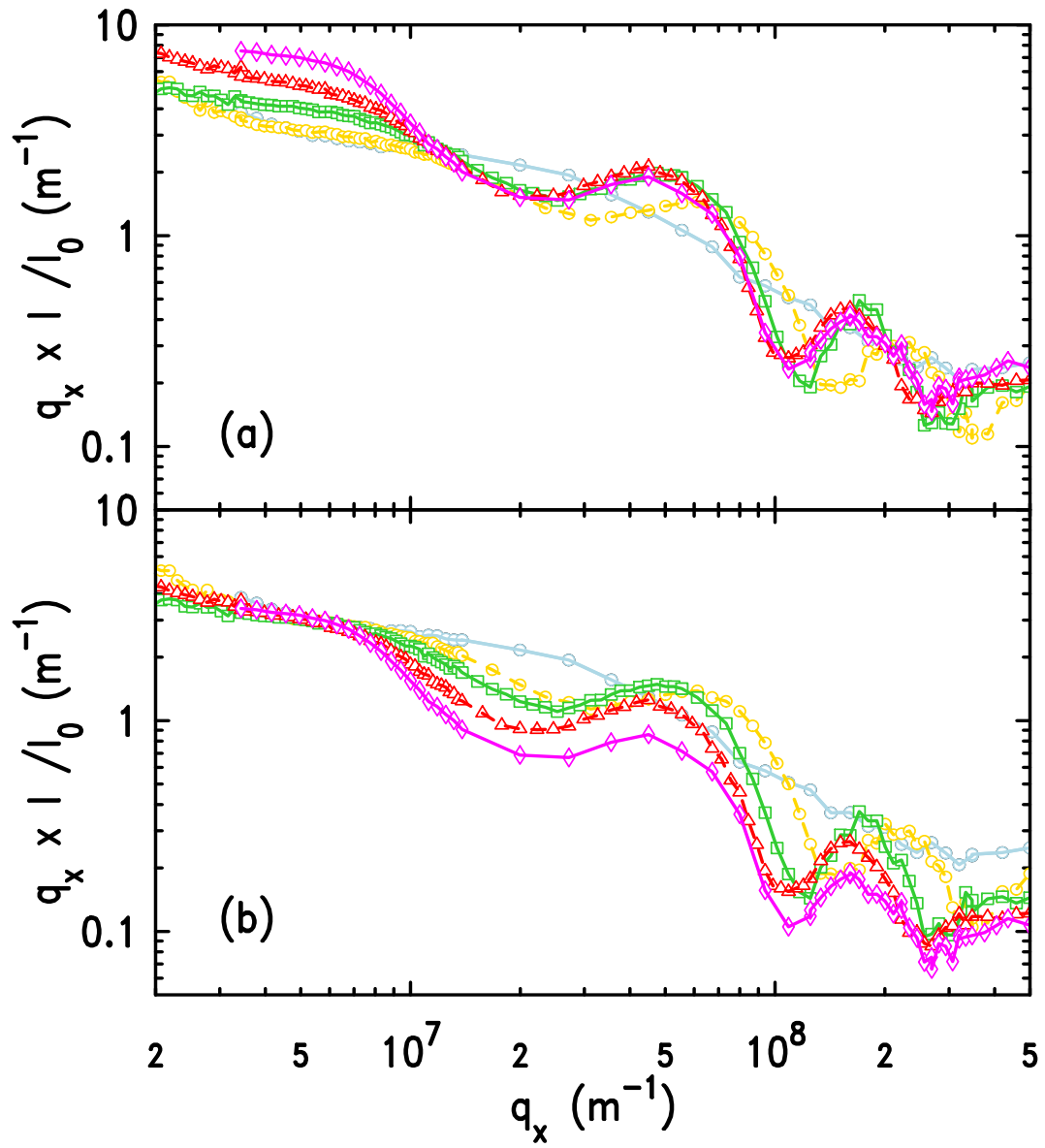


Fig. 3

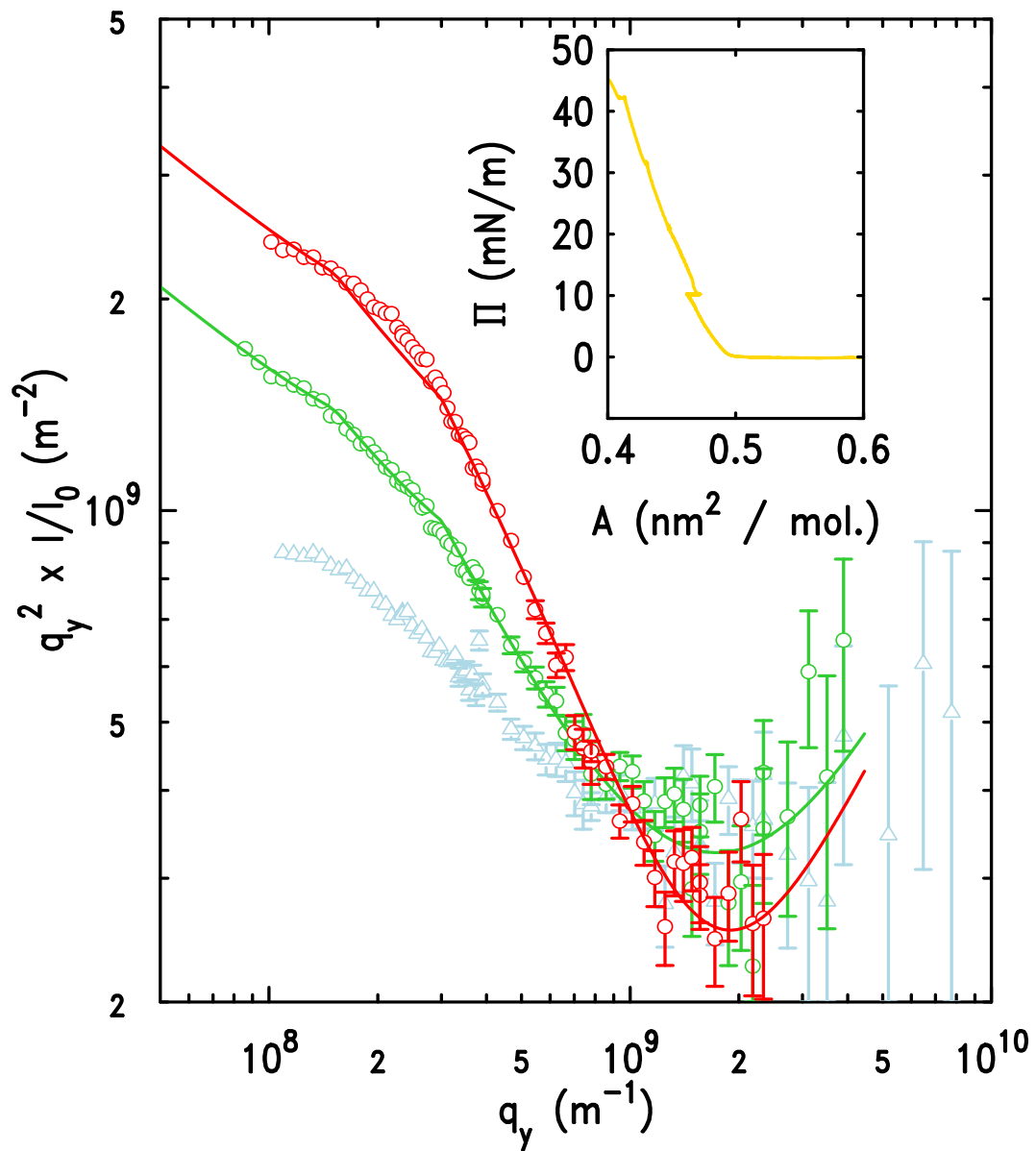


Fig. 4

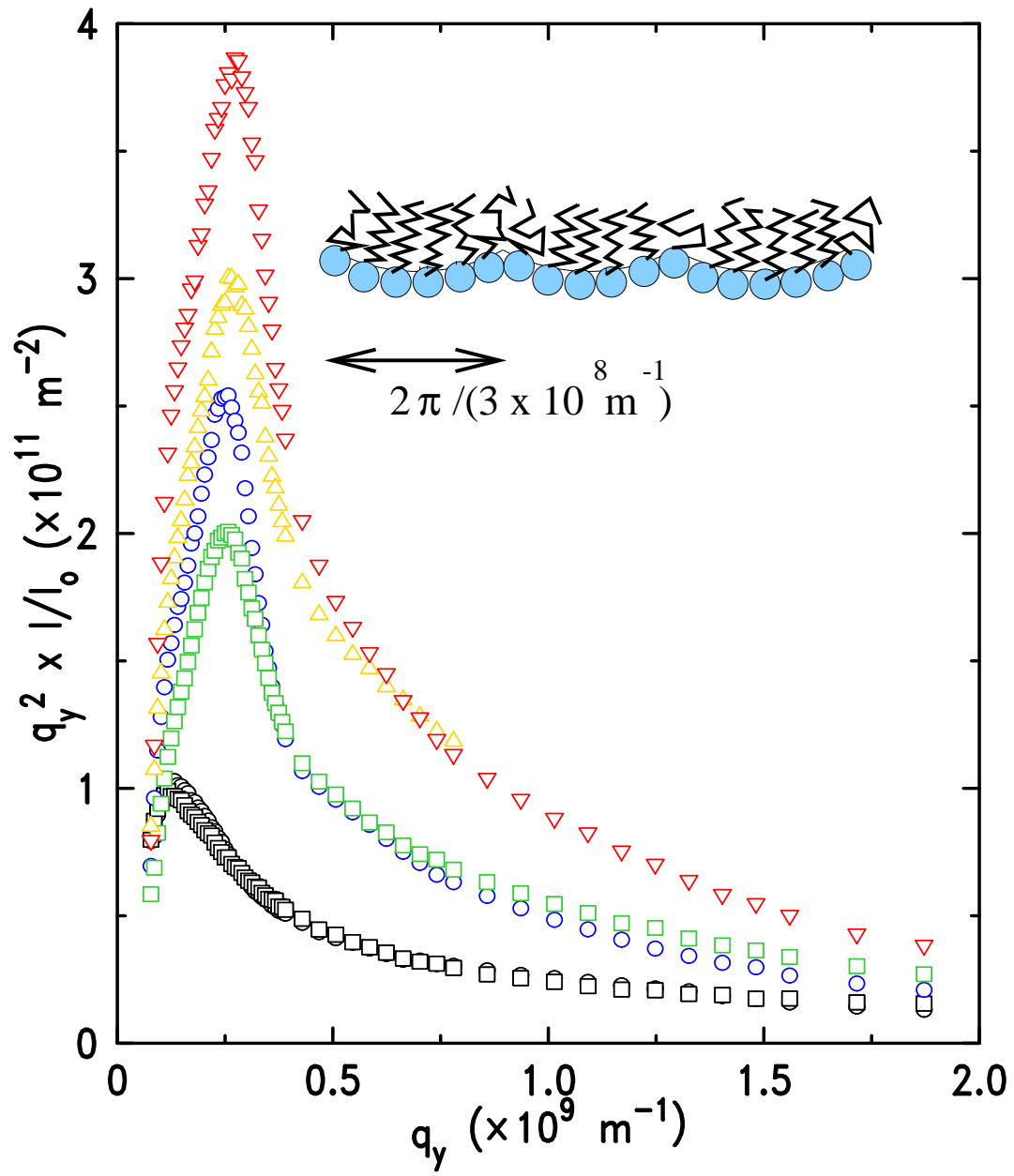


Fig. 5